Scheme III[7]

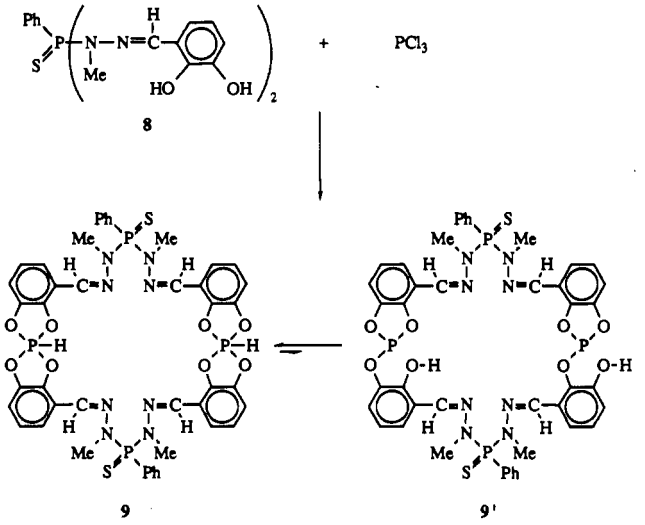

phosphorus, and the large coupling constant suggested a direct P–H bond.[6] Low-temperature spectra clearly confirmed the existence of a P_{III} (δ = 132.9) $\rightleftarrows$ P_V (δ = −19) equilibrium, the intensity of the signal at 132.9 ppm dramatically increased with the temperature, while the signal at −19 ppm decreased simultaneously in the same proportion. No change was observed for the signal due to the P_{IV} fragment (δ = 79). The above data are in agreement with the existence of an equilibrium between species **9** and **9'** (Scheme III). Further support for these formulations was obtained from a molecular weight determination (mass spectrometry), indicating that a [2 + 2] condensation reaction had taken place (as described in Schemes I and II).

Studies of the chemical properties of these macrocycles are underway.

Supplementary Material Available: A table of CHN analyses of compounds **5a,b**, **6a,b**, **7a–h**, and **9** (1 page). Ordering information is given on any current masthead page.

(6) Tebby, J. C. In *Phosphorus-31 NMR Spectroscopy in Stereochemical Analysis*; Verkade, J. G., Quin, L. D., Eds.; VCH: Deerfield Beach, FL, 1987; Chapter 1.
(7) **9'** is one of the possible isomers arising from the migration of the proton from phosphorus to oxygen.

Laboratoire de Chimie de Coordination du CNRS
UPR 8241 liée par conventions à l'Université Paul Sabatier et à l'Institut National Polytechnique de Toulouse
205 route de Narbonne
31077 Toulouse Cedex, France

Dominique Colombo
Anne-Marie Caminade
Jean Pierre Majoral*

Received February 28, 1991

Magnetic Phase Diagram of the Hole-Doped T' Phases $Nd_{2-x}Sr_xCuO_{4-\delta}$

The contrast in magnetic behavior with increasing dopant concentration between the hole carrier $La_{2-x}Sr_xCuO_{4-\delta}$[1] and the electron carrier $Nd_{2-x}Ce_xCuO_{4-\delta}$[2] systems illustrates the complex interplay between magnetism and superconductivity in the cuprate high T_c materials.[3] Electron doping in $Nd_{2-x}Ce_xCuO_{4-\delta}$ has a much less marked effect on T_N and the staggered moment on the Cu(II) sublattice than hole doping in $La_{2-x}Sr_xCuO_{4-\delta}$, which rapidly destroys the Néel state.[4,5] This is due to the less pronounced effect on magnetic long-range order (LRO) of dilution[6-9] by nonmagnetic Cu^I states compared to frustration arising from competing superexchange interactions from[4] O^- or[5] Cu^{III} states formed on hole doping. In both systems, the antiferromagnetic instability is removed before the onset of superconductivity.

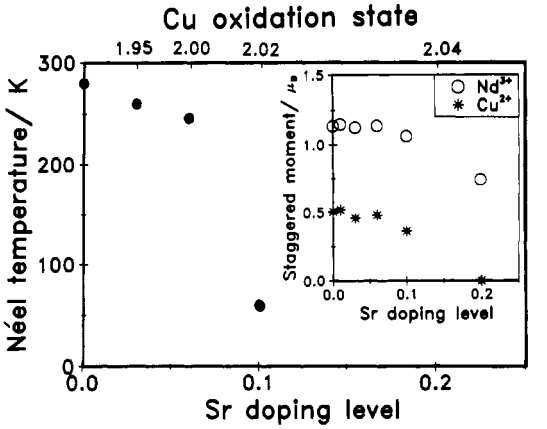

Figure 1. Néel temperature (K) for LR Cu antiferromagnetic order as a function of dopant concentration in $Nd_{2-x}Sr_xCuO_{4-\delta}$, determined by the μSR experiments. The x = 0.2 composition shows no evidence for an oscillation signal. Inset: Composition dependence of the staggered moments (μ_B) on the Cu and Nd sublattices at 1.5 K, determined by powder neutron diffraction.

Table I. Oxygen Concentration, Formal Cu Oxidation State, and Cu Moment (at 1.5 K) in $Nd_{2-x}Sr_xCuO_{4-\delta}$

x	δ	Cu oxidn state	μ_{Cu}/μ_B
0.03	0.04	+1.95	0.46 (2)
0.06	0.03	+2.00	0.48 (1)
0.10	0.04	+2.02	0.36 (8)
0.20	0.08	+2.04	0.0

In view of the differing magnetic behavior on hole and electron doping, it is important to note that, thus far, successful hole and electron doping of the same parent material, leading to superconductivity, has yet to be achieved. In the case of the K_2NiF_4 (O) and T' structures, the tolerance factors[10,11] control the range of formal Cu oxidation states that the structures are compatible with. In this communication, we report on our attempts to achieve hole doping of the T' phase and the magnetic properties of the $Nd_{2-x}Sr_xCuO_{4-\delta}$ (x = 0.00–0.20) system, studied by zero-field longitudinal-geometry muon spin relaxation and powder neutron diffraction.

$Nd_{2-x}Sr_xCuO_{4-\delta}$ compositions (x = 0.03, 0.06, 0.10) were synthesized by the citrate sol–gel technique;[10,12] $Nd_{1.9}Sr_{0.1}CuO_{4-\delta}$

(1) Bednorz, J. G.; Muller, K. A. *Z. Phys. B* **1986**, *64*, 189–193.
(2) Tokura, Y.; Takagi, H.; Uchida, S. *Nature* **1989**, *337*, 345–347.
(3) Rosseinsky, M. J.; Prassides, K.; Day, P. *J. Chem. Soc., Chem. Commun.* **1989**, 1734–1736. Rosseinsky, M. J.; Prassides, K. *Physica C* **1989**, *162*–164, 522–523. Rosseinsky, M. J.; Prassides, K. *Physica B* **1990**, *165&166*, 1187–1188.
(4) Birgeneau, R. J.; Kastner, M. A.; Aharony, A. *Z. Phys. B* **1988**, *71*, 57–62.
(5) Rosseinsky, M. J.; Prassides, K.; Day, P. *J. Mater. Chem.* **1991**, *1*, 597–610.
(6) Rosseinsky, M. J.; Prassides, K.; Day, P. *Inorg. Chem.* **1991**, *30*, 2680–2687.
(7) Luke, G. M.; et al. *Nature* **1989**, *338*, 49–51.
(8) Yamada, K.; Kakurai, K.; Endoh, Y. *Physica C* **1990**, *165*, 131–132. Endoh, Y.; Matsuda, M.; Yamada, K.; Kakurai, K.; Hidaka, Y.; Shirane, G.; Birgeneau, R. J. *Phys. Rev. B* **1989**, *40*, 7023–7026. Matsuda, M.; Yamada, K.; Kakurai, K.; Kadowski, H.; Thurston, T. R.; Endoh, Y.; Hidaka, Y.; Birgeneau, R. J.; Gehring, P. M.; Moudden, A. H.; Shirane, G. *Phys. Rev. B*, in press. Skanthakumar, S.; Zhang, H.; Clinton, T. W.; Li, W.-H.; Lynn, J. W.; Fisk, Z.; Cheong, S.-W. *Physica C* **1989**, *160*, 124–128.
(9) Luke, G. M.; et al. *Physica C* **1989**, *162*–164, 825–826. Luke, G. M.; et al. *Phys. Rev. B* **1990**, *42*, 7981–7988.
(10) Rosseinsky, M. J.; Prassides, K.; Day, P. *Physica C* **1989**, *161*, 21–33.
(11) Goodenough, J. B. *Supercond. Sci. Technol.* **1990**, *3*, 26–37.
(12) Wang, H. H.; Geiser, U.; Thorn, R. J.; Carlson, K. D.; Beno, M. A.; Monaghan, M. R.; Allan, T. J.; Proksch, R. B.; Stupka, D. L.; Kwok, W. K.; Crabtree, G. W.; Williams, J. M. *Inorg. Chem.* **1987**, *26*, 1190–1192.

0020-1669/91/1330-3367$02.50/0

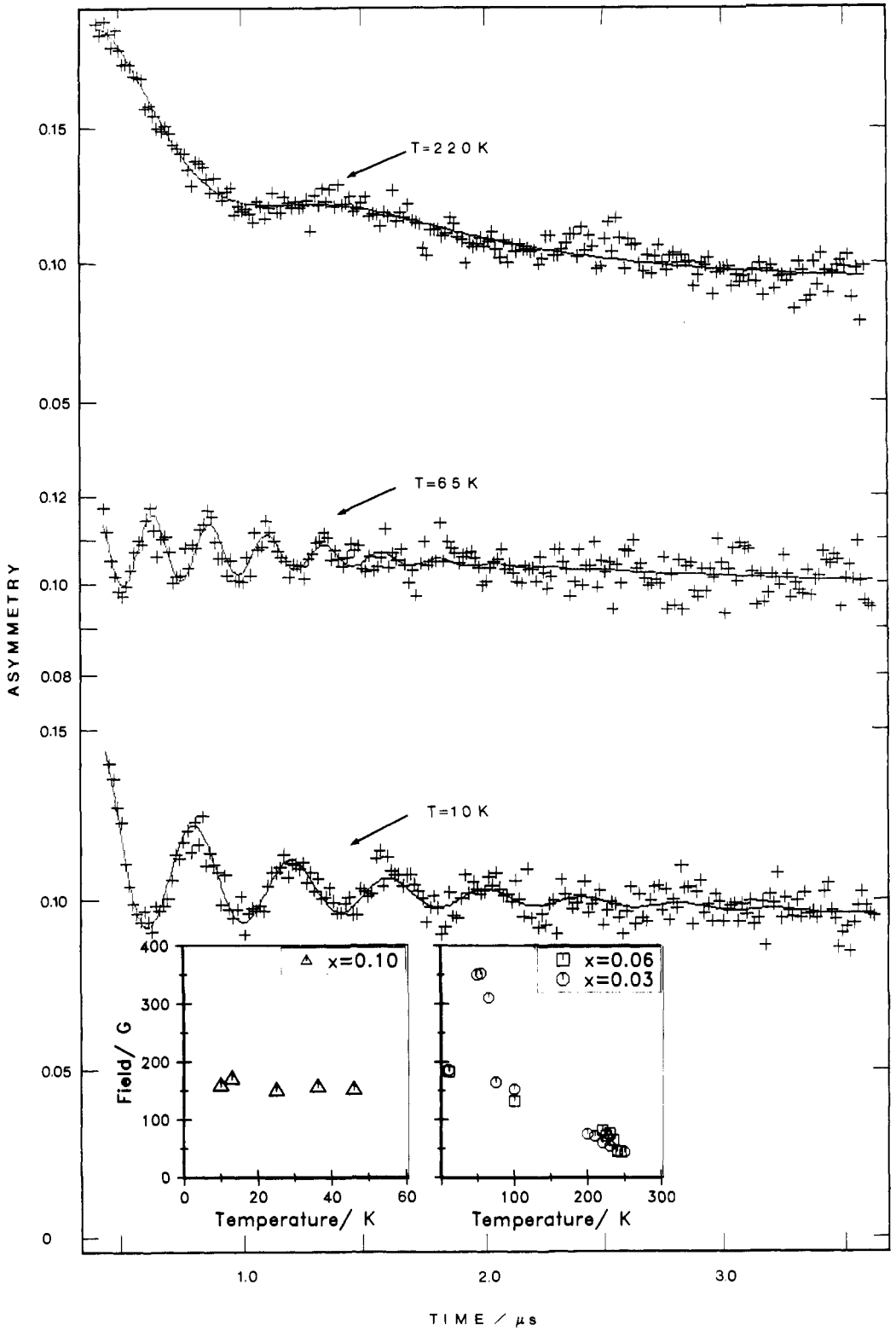

Figure 2. Zero-field precession signal in $Nd_{1.97}Sr_{0.03}CuO_{3.96}$, which is indicative of a magnetically ordered state at 220, 65, and 10 K. The temperature evolution of the signal shows the presence of two successive spin reorientation transitions. Inset: Temperature evolution of the local fields at the muon sites (G) for the samples with x = 0.03, 0.06, and 0.10.

was further annealed at 650 °C in an oxygen flow. Earlier studies[13] had reported that the solubility limit for strontium was near x = 0.10. However, we prepared $Nd_{1.8}Sr_{0.2}CuO_{4-\delta}$ by decomposing the citrate powder in air at 650 °C for 24 h in a platinum crucible followed by quenching to room temperature. Phase purity was confirmed by powder X-ray diffraction.[14] The oxygen concentrations were evaluated by thermogravimetric reduction,[6] and the formal Cu oxidation state was determined by iodometric titration.[15] Zero-field μSR experiments were performed in longitudinal geometry[16] between 10 K and room temperature by using the pulsed muon facility[17] at the Rutherford Appleton Laboratory, Didcot, U.K. Spin-polarized positive muons are implanted at interstitial sites and precess in the local magnetic field at a frequency of $\omega = \gamma_\mu B_{loc}$ ($\gamma_\mu/2\pi$ = 13.55 kHz/G). Relaxation of the μ^+ polarization is monitored by detecting the

(13) Gopalakrishnan, J.; Subramanian, M. A.; Torardi, C. C.; Attfield, P.; Sleight, A. W. *Mater. Res. Bull.* **1989**, *24*, 321.

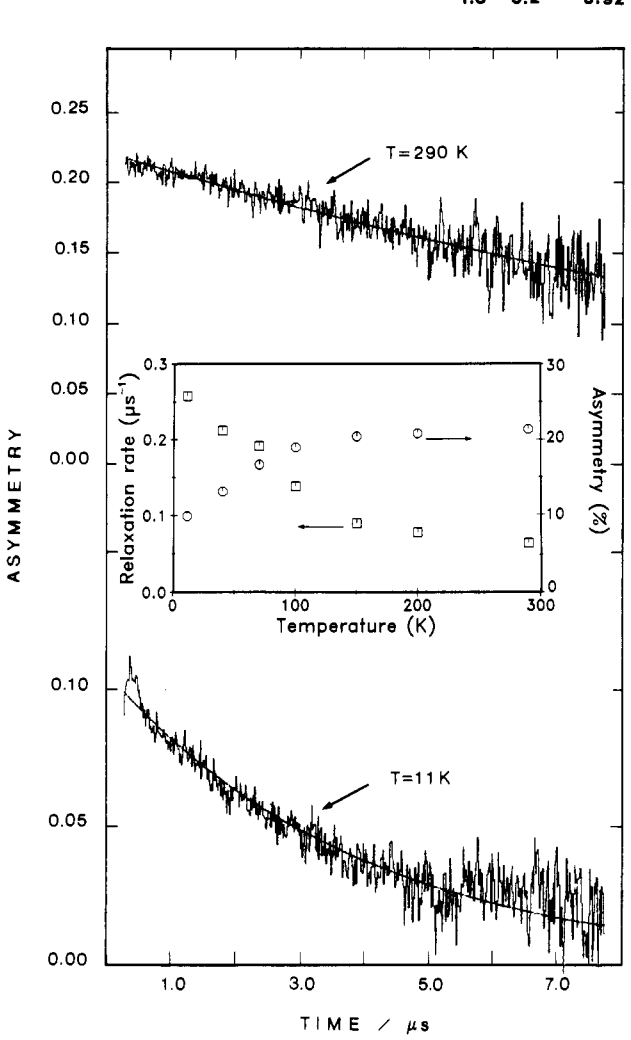

Figure 3. Zero-field μSR spectra for $Nd_{1.80}Sr_{0.20}CuO_{3.92}$ at 11 and 290 K fitted to Lorentzian decays. Inset: Temperature evolution of initial asymmetry A_0 (%) and relaxation rate λ (μs^{-1}) for the same sample.

decay positrons emitted preferentially along the muon spin direction. Data are shown as the asymmetry $A(t) = [B(t) - \alpha F(t)]/[B(t) + \alpha F(t)]$, where B and F refer to the number of positrons detected behind and in front of the sample[16] and α is a normalization constant obtained from preliminary calibration using a weak (20 G) transverse field.[18] Powder neutron diffraction data were collected between 1.5 K and room temperature on the D1b powder diffractometer[19] at the Institut Laue Langevin, Grenoble, France, using neutrons with a mean wavelength of 2.522 Å.

Table I shows that hole doping of the CuO_2 layers is achieved only for $x = 0.1$ (2%) and $x = 0.2$ (4%) doping. This is supported by the zero-field μSR results for the $x \leq 0.06$ samples, where the Néel temperatures, determined by the onset of oscillations in the asymmetry, are similar to that of Nd_2CuO_4 (Figure 1).[7] Figure 2 shows the zero-field asymmetry for $Nd_{1.97}Sr_{0.03}CuO_{3.96}$ at 220, 65, and 10 K. The spin reorientation transition from La_2NiO_4- to La_2CuO_4-type magnetic structures, found for 35 K < T < 75 K in Nd_2CuO_4,[8] is seen as a large increase in the muon internal field[9] from 164 (3) G at 75 K to 309 (3) G at 65 K; this is followed on cooling by a return to local field values (B_μ = 186 (2) G) characteristic of the high-temperature magnetic structure (Figure 2, inset). We also observe an increase in the relaxation rate at 100 K (λ = 4.6 (3) μs^{-1}), which we interpret as a precursor to the spin reorientation transition. For the $x = 0.06$ sample, the onset of oscillations in the asymmetry[20] occurs at ca. 240 K. At lower temperatures, data were recorded only at 10 and 100 K. The temperature evolution of the local fields at the muon sites is also shown in Figure 2 (inset). Study of the 1.5 K neutron diffraction profiles of the samples with $x = 0.01$, 0.03, and 0.06 revealed the presence of seven magnetic peaks, which could be indexed on the basis of a $2^{1/2} \times 2^{1/2}$ rotation of the basal plane of the *I*4/*mmm* unit cell. The magnetic structure (magnetic space group $F'_Amm'm'$) is identical with the one determined for the parent Nd_2CuO_4 compound and its electron-doped analogues.[3,6,21] The values of the staggered magnetic moments on the Cu sublattice at 1.5 K (Table I) are similar to the value of 0.507 (3) μ_B found for Nd_2CuO_4.[3,6] The Sr^{2+} doping level dependence of the staggered moments for both the Nd^{3+} and the Cu^{2+} sublattices is included in Figure 1 (inset).

A marked change in behavior is observed at higher Sr^{2+} concentrations. The 2% hole doping ($Nd_{1.9}Sr_{0.1}CuO_{3.96}$) sharply reduces the Néel temperature to ca. 60 K (Figure 1) and removes the spin reorientation transition. The evolution of the local field at the muon site with temperature (Figure 2, inset) shows no significant changes in the 10–60 K range. Furthermore, integrated intensity analysis of the magnetic neutron diffraction data shows that μ_{Cu} = 0.36 (8) μ_B and μ_{Nd} = 1.06 (6) μ_B at 1.5 K. The Néel state is further disrupted as the Cu oxidation state increases to +2.04 in $Nd_{1.8}Sr_{0.2}CuO_{3.92}$. No oscillations characteristic of antiferromagnetic LRO are observed in the asymmetry down to 11 K (Figure 3), and no moment is detected on the Cu sublattice

(14) The powder neutron diffraction profile of $Nd_{1.94}Sr_{0.06}CuO_4$ has been recorded at room temperature on the High Resolution Powder Diffractometer (HRPD) at the ISIS pulsed neutron source, Rutherford Appleton Laboratory, with the sample in the 1-m position over a d-spacing range of 0.6–2.6 Å. A Rietveld profile refinement was carried out successfully in the teragonal *I*4/*mmm* space group (T' phase). The structural results as well as the temperature evolution of the resistivity for this sample have been already reported in ref 10. The results of the structural analyses of the other samples in this series will be published in detail elsewhere.

(15) Nazzal, A. I.; Lee, V. Y.; Engler, E. M.; Jacowitz, R. D.; Tokura, Y.; Torrance, J. B. *Physica C* **1988**, *153–155*, 1367–1368.

(16) Cox, S. F. J. *J. Phys. C: Solid State Phys.* **1987**, *20*, 3187–3199.

(17) Eaton, G. H.; Carne, A.; Cox, S. F. J.; Davies, J. D.; de Renzi, R.; Hartmann, O.; Kratzer, A.; Ristori, C.; Scott, C. A.; Stirling, G. C.; Sundqvist, T. *Nucl. Instrum. Methods Phys. Res., Sect. A* **1988**, *269*, 483–491.

(18) Static moments in a magnetically ordered material have a narrow local field distribution, causing coherent precession of the muon magnetization, which produces oscillations in the asymmetry. Frozen or disordered static moments produce rapid relaxation of the polarization and no oscillations. Dynamic relaxation by rapidly fluctuating moments in a dense spin system gives rise to the exponential (Lorentzian) relaxation function $A(t) = A_0 \exp(-\lambda t)$, where $\lambda = T_1^{-1} \sim \langle\omega^2\rangle\tau_c$ and τ_c is the spin fluctuation correlation time ($\langle B(t)B(0)\rangle \propto \exp(-t/\tau_c)$); hence, rapid fluctuations give slow relaxation due to motional averaging over the local field distribution $\langle\omega^2\rangle$. Slowly fluctuating moments ($\tau_c^{-1} < \omega$) produce relaxation that, at short times, resembles that due to random static moments, with an initial dip in the asymmetry at short t (Kubo–Toyabe function: Kubo, R. *Phys. Rev. B* **1979**, *20*, 850). However, the asymmetry recovers to a constant value ($\sim A_0/3$) for static fields, whereas continued decay at longer times is observed for fluctuating moments.

(19) Pannetier, J. *Chem. Scr. A* **1986**, *26*, 131–139.

(20) Data were collected between 235 and 247 K at 2 K intervals and between 220 and 235 K at 5 K intervals. There is no evidence for muon precession at 245 or 242 K. The observed local fields (Figure 2, inset) in the 220–240 K temperature range were fitted to the equation, $B_\mu(T) = B_\mu(0)(1 - T/T_N)^\beta$, where $B_\mu(0)$ was taken from the base temperature run. The critical exponent analysis gave β = 0.37 (3) and T_N = 246 (10) K. This result favors a 3D Heisenberg spin Hamiltonian close to the transition: de Jongh, L. J.; Miedema, A. P. *Adv. Phys.* **1974**, *23*, 1.

(21) In a manner similar to that observed for Nd_2CuO_4,[3,6] it is found that the Cu and Nd spins are constrained by symmetry to lie in the same direction ($^1/_2$, $^1/_2$, 0) and they are parallel to the magnetic propagation vector $\mathbf{k}$ = ($^1/_2$, $^1/_2$, 0). An integrated intensity analysis of the five most intense magnetic peaks was performed, resulting in μ_{Cu} = 0.52 (5), 0.46 (2) and 0.48 (1) μ_B and μ_{Nd} = 1.150 (8), 1.126 (4), and 1.138 (4) μ_B for the x = 0.01, 0.03, and 0.06 samples, respectively. The form factor for Cu was obtained by interpolation from the measurements of Freltoft et al. (*Phys. Rev. B* **1988**, *37*, 137) and the Nd form factor was calculated in the dipolar approximation from the relativistic calculations of Freeman and Desclaux (*J. Magn. Magn. Mater.* **1979**, *12*, 4). The magnetic intensity was scaled to the intensities of the nuclear (002) and (202) peaks. The results of these analyses will be published in detail elsewhere.

at 1.5 K by powder neutron diffraction.[22] The observed asymmetry in the ZF μSR spectra is well fitted to a single Lorentzian decay [$A = A_0 \exp(-\lambda t)$] over all temperatures studied (11–290 K). The variation of the initial asymmetry A_0 and the relaxation rate λ with temperature is shown in Figure 3 (inset). The decrease in the asymmetry begins at the same temperature ($\sim$100 K) that the relaxation rate begins to increase. The initial asymmetry at 11 K (A_0 = 9.92 (7)%) is less than half its room temperature value (A_0 = 21.34 (9)%), with an extrapolated 0 K value of $\sim(1/3)A_0(RT)$. The spin glass system $Fe_{2-x}Ti_{1+x}O_5$ shows a divergence in λ and reduction of A_0 to $^1/_3$ below the freezing transition,[23] and our observations are consistent with a significant slowing of the spin fluctuations below 70 K. The relaxation rate is still increasing at 11 K (λ = 0.258 (4) μs^{-1}), indicating that the slowing down is incomplete, and we have not directly observed static moments, only slowly fluctuating ones.[24] The sharp decrease of the initial asymmetry A_0 suggests a contribution from static moments,[26] as the data do not extend to short enough times to allow the observation of highly damped oscillations or Kubo–Toyabe line shapes of the type reported for $La_{1.94}Sr_{0.06}CuO_4$.[25] In the latter case, spin freezing at 6 K is followed by Kubo–Toyabe behavior at 3.9 K. μSR measurements to lower temperatures and shorter times, plus longitudinal field μSR, are required to unambiguously separate static from dynamic contributions.

In conclusion, samples in the $Nd_{2-x}Sr_xCuO_{4-\delta}$ system with a formal copper oxidation state of less than II show magnetic behavior similar to that observed for undoped Nd_2CuO_4. However, the formally oxidized $Nd_{1.9}Sr_{0.1}CuO_{3.96}$ and $Nd_{1.8}Sr_{0.2}CuO_{3.92}$, though displaying activated conductivity, show magnetic behavior similar to that found with increasing hole concentration in $La_{2-x}Sr_xCuO_{4-\delta}$; the Néel temperature first decreases (x = 0.1, 2% holes), and then magnetic LRO disappears as a frustrated spin-glass state is formed (x = 0.2, 4% holes). In both oxidized samples, spin fluctuations in the paramagnetic state seem significantly slowed relative to the unoxidized materials, producing significant relaxation at $T > T_N$. Hence, it appears that the destruction of magnetic LRO is a necessary but not sufficient condition for the onset of metallic and superconducting behavior: ϵ_F lies below the mobility edge when T_N goes to zero in $La_{2-x}Sr_xCuO_{4-\delta}$. The contrast with the $Nd_{2-x}Ce_xCuO_{4-\delta}$ system shows that localized holes, before the metal–insulator transition, can frustrate magnetic order but localized electrons can only dilute the Cu^{2+} moment, requiring delocalization to allow double exchange to give the required frustration. The larger Cu–O bond lengths in the T′ structure allow hole trapping at higher hole concentrations and combine with the crystal chemistry to drive the Sr^{2+} concentration required for the metal–insulator transition *above the solubility limit of* Sr^{2+} *in* Nd_2CuO_4.

Acknowledgment. We thank the SERC for financial support of this work, the Rutherford Appleton Laboratory and the Institut Laue Langevin for provision of muon and neutron time, and Dr. Roberto de Renzi (Parma, Italy) for providing the MUZEN programme used in the analysis of muon data. M.J.R. thanks Merton College, Oxford University, for a Junior Research Fellowship.

(22) The Nd staggered moment is 0.74 (6) μ_B at 1.5 K for the x = 0.2 sample.
(23) Boekema, C.; Brabers, V. A. M.; Lichti, R. L.; Denison, A. B.; Cooke, D. W.; Heffner, R. H.; Hutson, R. L.; Schillaci, M. E.; MacLaughlin, D. E.; Dodds, S. A. *Hyperfine Interact.* **1986**, *31*, 369.
(24) A rough estimate of the fluctuation frequency ν at 11 K may be obtained[18,25] by taking the local field strength B in this sample as $\sim$180 G and λ(11 K) = 0.258 (4) μs^{-1}; then, $\nu \sim 10^9$ Hz.
(25) Sternlieb, B. J.; et al. *Phys. Rev. B* **1990**, *41*, 8866.
(26) Kitazawa, H.; Katsumata, K.; Torikai, E.; Nagamine, K. *Solid State Commun.* **1988**, *67*, 1191.
(27) To whom correspondence should be addressed.
(28) Present address: AT&T Bell Laboratories, Murray Hill, NJ 07974.

Inorganic Chemistry Laboratory — **Matthew J. Rosseinsky***,[27,28]
Oxford University
Oxford OX1 3QR, U.K.

School of Chemistry and Molecular Sciences — **Kosmas Prassides***,[27]
University of Sussex
Brighton BN1 9QJ, U.K.

Rutherford Appleton Laboratory — **Christopher A. Scott**
Didcot, Oxon OX11 0QX, U.K.

Received March 7, 1991